

Simulation 2D of the closure of an artificial  
Aortic Valve by blood reflux using Arbitrary  
Lagrangian Eulerian (ALE) Formulation.

Vincent MOREAU

07.07.97 updated 16.07.97

C.R.S. 4  
Via Nazario Sauro, 10  
09123 Cagliari, Italie

**Abstract**

We present the 2D simulation of the interaction of an artificial aortic valve and the blood reflux at the end of the systole. The valve is pivoting of 60 degrees under the flow pressure. The ALE formulation is used and mesh is regenerated periodically. Coupling procedures and mesh regeneration are described with care given to technical difficulties. Results are shown and commented underlining their limits and potentiality.

# 1 Introduction

In the cardiac cycle, at the end of the systole, the reflux of blood from the aorta to the left ventricle is stopped by the closure of the aortic valve. If the natural aortic valve gets damaged, a now common procedure is to replace it by a prosthesis. There are many design for artificial valves; in this study, we have considered the bileaflet model by Sorin ([11]). The aortic valves, both natural and artificial, are passive objects where opening and closing phase are governed solely by the blood flow. Points of interest in the analysis of an artificial valve are:

1. **the maximum shear rate** to evaluate the risk of hemolise,
2. **the blood reflux volume** to measure its efficiency and
3. **the closing velocity** to estimate the possible weaving of the valve material.

Numerical simulation is done using an ALE formulation for the fluid, allowing moving domains. The blood is considered to be incompressible and Newtonian. It is governed by the Navier-Stokes equations. The valve is supposed to be rigid with two symmetric leaflets that rotates over a fixed axis. Only half of the domain is simulated. Doing a 2D planar simulation, we don't pretend to obtain meaningful quantitative results but only to indicate an approach to the problem that will give quantitative data in the future 3D simulation.

The fluid is transferring its pressure to the structure which in turn transfers its displacement to the fluid. Geometry changes drastically during the simulation, so remeshing is done when necessary. We give results of the simulations and show that some interesting results can already be inferred with such a basic approximation. Other works have been done on the flow around a cardiac valve. We refer to King and al. (1996) ([15]) for a quite complete bibliography, both experimental and numerical. Apart from Peskin & al. (1992) ([16]), for the mitral valve, we do not know of any other direct simulation with a moving boundary.

## 2 Notations and Constitutive Equations

Our domain  $\Omega$  is composed of two parts evolving in time:

1.  $\Omega_f$  for the fluid domain,
2.  $\Omega_l$  for the leaflet.

Technically our domain of simulation is defined by five boundaries:

1.  $\Gamma_i$  where the inlet flow is prescribed,
2.  $\Gamma_o$  for the free (Neumann) outlet flow,

3.  $\Gamma_h$  for the fixed external wall with homogeneous Dirichlet conditions for the velocity,
4.  $\Gamma_m$  for the moving boundary, that is the leaflet boundary,
5.  $\Gamma_s$  for the symmetry axe.

There are two geometrical points of interest:

1.  $C_G$  the leaflet center of inertia,
2.  $C_R$  the leaflet center of rotation.

When the center of rotation is not fixed in time, it follows a path linked to the inclination of the leaflet:

1.  $\Gamma_r$  is the trajectory of the center of rotation.

These informations are illustrated in figure (1).

## 2.1 Leaflet equations

The leaflet momentum  $M_F$  about the point  $C_R$ , is calculated from the pressure and viscous forces applied by the fluid, and it is used to calculate the leaflet angular acceleration, velocity and position after one time step  $Dt$ . We have:

$$M_F = \int_{\Gamma_m} [(PI + \nu \nabla u) \cdot n] \wedge \overrightarrow{C_R X} dX \quad (1)$$

where  $P$  is the pressure,  $I$  the identity matrix,  $u$  the fluid velocity and  $n$  is the normal pointing outside the fluid domain.

The inertial moment of the leaflet about  $C_R$ ,  $M_{iR}$  is given by:

$$M_{iR} = M_{iG} + m_l \cdot |C_G C_R|^2 \quad (2)$$

where  $m_l$  is the total mass of the leaflet and  $|C_G C_R|$  is the distance between the two points  $C_G$  and  $C_R$ . We have used  $M_{iG}$  the inertial moment of the leaflet about its center of inertia  $C_G$  which is defined, knowing  $\rho_l$  the leaflet density, by:

$$M_{iG} = \int_{\Omega_w} \rho_l |GX|^2. \quad (3)$$

The angular acceleration  $\ddot{\theta}$  is then calculated by:

$$\ddot{\theta} = \frac{M_F}{|C_G C_R| \cdot M_{iG}} \quad (4)$$

to give angular velocity and value as:

$$\dot{\theta}(n+1) = \dot{\theta}(n) + Dt \cdot \ddot{\theta}, \quad (5)$$

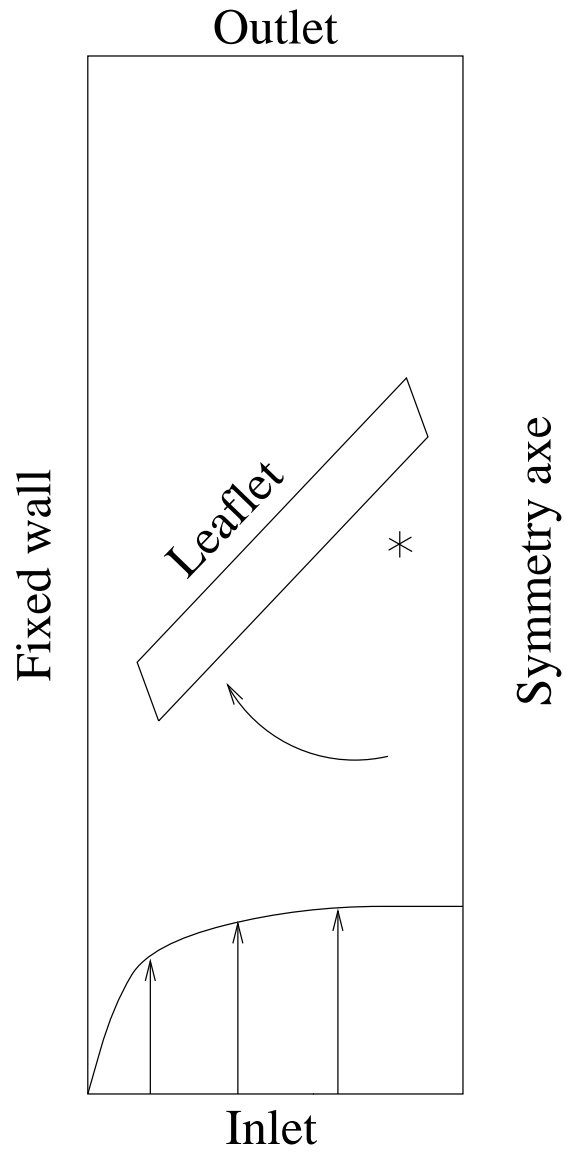


Figure 1: Scheme of the geometry with the velocity profile in inlet and the sens of rotation of the valve leaflet.

$$\theta(n+1) = \theta(n) + \frac{Dt}{2} \cdot (\dot{\theta}(n+1) + \dot{\theta}(n)). \quad (6)$$

The new position  $X^{n+1}$  of a point  $M$  of the leaflet boundary is known from its previous position  $X^n$ , the angle associated  $\theta_M(X^n)$ , and the angular increment. Noting:

$$X^{n+1} = \theta_M^{-1}(\theta_M(X^n) + \theta^{n+1} - \theta^n). \quad (7)$$

The velocity of the leaflet, which is also the boundary velocity both for the mesh and the fluid is finally computed by:

$$u_l = \frac{\overrightarrow{X^n X^{n+1}}}{Dt}. \quad (8)$$

## 2.2 Fluid equations

The fluid is governed by the incompressible Navier-Stokes equations:

$$\begin{cases} \partial_t u + (u \cdot \nabla) u - \nu \Delta u + \nabla P = 0 & \text{in } \Omega_f(t) \\ \nabla \cdot u = 0 \end{cases} \quad (9)$$

where  $u$  is the fluid velocity,  $P$  its pressure and  $\nu$  its viscosity.

To overcome the difficulty coming from the change of  $\Omega_f$  during one time step, we fix the domain for that time step and transport the equation over the fixed domain. We obtain the following formulation ([5],[1],[2], [3], [6], [7]), known as the Arbitrary Lagrangian Eulerian (ALE) formulation:

$$\begin{cases} \partial_t \tilde{u} + ([\tilde{u} - c] \cdot \nabla) \tilde{u} - \nu \Delta \tilde{u} + \nabla \tilde{P} = 0 & \text{in } \tilde{\Omega}_f([t_n, t_{n+1}]) = \Omega_f(t_{n+1}), \\ \nabla \cdot \tilde{u} = 0 \end{cases} \quad (10)$$

where  $c$  is the domain velocity and will serve as mesh velocity.  $\tilde{P}$  and  $\tilde{u}$  are first order approximations in  $Dt$  of the previous pressure and velocity ([8], [4]). This system is completed by the following boundary conditions:

$$\begin{cases} \tilde{u} = g & \text{(given) on } \Gamma_i, \\ \tilde{u} = 0 & \text{on } \Gamma_h, \\ u = u_l & \text{on } \Gamma_m, \\ \nabla \tilde{P} \cdot n = 0 & \text{on } \Gamma_i \cup \Gamma_h \cup \Gamma_m, \\ \tilde{P} = 0 & \text{on } \Gamma_o. \end{cases} \quad (11)$$

with  $u_l$  is the leaflet velocity and constitute the coupling term.

From now on, we will drop the tilde “ $\tilde{\phantom{x}}$ ” for the sake of simplicity.

We present briefly the numerical scheme for the fluid which uses operator splitting and projection methods. It is implemented in the N3S software by Simulog. Knowing  $u$ ,  $P$  and  $c$  at time  $n$ , along with the boundary Dirichlet conditions and positions at step  $n+1$ , we want to compute the variables at time  $n+1$ .

1. First Step: Compute the domain velocity, solving a Laplace problem and transport the mesh on the domain at time  $n + 1$ .
2. Second Step: Convection of the velocity field, by a characteristics method. Roughly equivalent to giving an intermediary velocity solution  $u^{n+\frac{1}{2}}$  of:

$$u^{n+\frac{1}{2}} = u^n + Dt.([u^n - c].\nabla)u^n. \quad (12)$$

3. Third Step: Diffusion with Projection on the divergence free space, solving the system:

$$\begin{cases} \Delta P^{n+1} = \frac{\nabla \cdot u^{n+\frac{1}{2}}}{Dt} \\ u^{n+1} - \nu Dt. \Delta u^{n+1} = u^n - Dt. \nabla P^{n+1}. \end{cases} \quad (13)$$

### 3 Remeshing and interpolation

During the closure of the leaflet, there are regions where the mesh is evolving considerably with a decrease in mesh quality. We have chosen a strategy consisting in remeshing the whole domain as soon as the mesh quality reaches a fixed value of a mesh quality indicator  $Q_m$ . We define the quality  $Q_t$  of a triangle  $ABC$  in the following way:

$$Q_t = C \frac{\overrightarrow{AB} \wedge \overrightarrow{BC}}{|AB|^2 + |BC|^2 + |CA|^2} \quad (14)$$

where  $C = 2\sqrt{3}$  such that for an equilateral triangle  $Q_t = 1$ .

Please note that triangles have been given a “counterclockwise” orientation and the formula gives negative values when triangles are inverted.

The global quality  $Q_m$  of the mesh is defined as the minimum quality of all its triangles. It is checked at each iteration. When the quality criteria fails, a new mesh is computed on the geometry independently of the previous one (in fact we are preserving at present the mesh boundary structure). Then the velocity and pressure fields are computed by linearly interpolating the values at the new nodes over the old mesh node values. This interpolation is first order accurate (in space) and does not preserve the incompressibility constraint. This constraint is reestablished at the cost of a large, unphysical variation of pressure immediately after remeshing. This jump of pressure vanishes rapidly when the deformation of the geometry is enforced externally but can be source of strong long living instabilities when the pressure value is used to move the boundary, as in coupled problems. For this reason, we need to damp-out the pressure oscillation and the angular acceleration, after a remeshing is calculated for a few time step as a weighting between the angular acceleration before remeshing  $\ddot{\theta}(n_0)$  and the one caused by the actual pressure field  $\ddot{\theta}$  with the following formula:

$$\ddot{\theta}(n_0 + i) = \ddot{\theta}(n_0).e^{-\frac{i-1}{N}} + \ddot{\theta}(n_0 + i).(1 - e^{-\frac{i-1}{N}}) \quad (15)$$

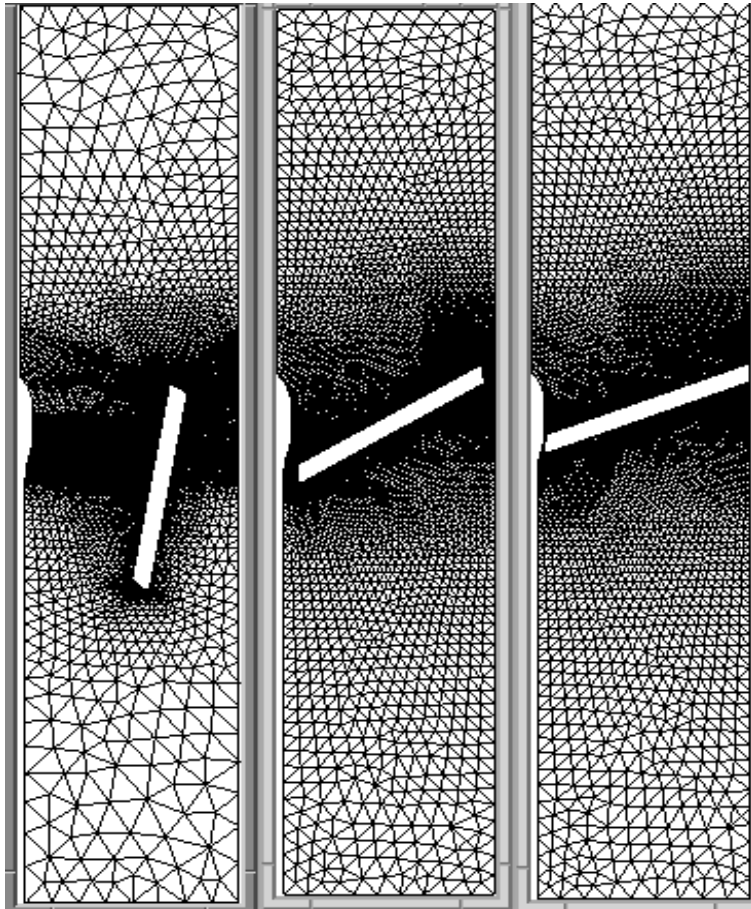


Figure 2: P1 structure of the mesh at the beginning, during and near the end of the simulation.

where  $N = 1$  in the ultimate version. Moreover, we ignore the pressure torques calculated at the end of the first time step.

Our interpolation method has the advantage of been quite simple and fast, and is well suited for a large range of situations. Nevertheless, in our simulation we come close to a topological change of the geometry ( the valve closure). So, remeshing and interpolation are done more and more often during the simulation. There is a serious risk that the accumulation in the introduced error could denature the solution. It would be therefore interesting to implement other methods, more accurate. For an analysis of the different possibilities for the regeneration of a discrete computational scalar or vectorial field after remeshing, we refer to ([9]). The most efficient methods seem to be the minimization based ones. They are unfortunately quite heavy to implement.

Another, complementary, approach is the continuous monitoring of the mesh with local remeshing capability based on a geometrical dynamic minimization of the error. This kind of approach, while now quite common for stationary simulations is at its first steps in the highly un-stationary case ([12], [13]).

## 4 Pressure in ALE formulation

It has also been numerically experienced that pressure seems very badly represented when boundary accelerations are involved ([10]) so that the coupling with a boundary structure is very unstable. Fortunately the pressure behaves well when no acceleration of the boundary is present. To overcome the difficulty, ([10]) has developed a strategy that consists in splitting each structural time step in two fluid time steps. All the acceleration effects on the boundary in the structure time step are concentrated in the first fluid time step. The second fluid time step is done with no acceleration of the boundary (at first order, it is in fact the angular acceleration that is dealt with). The pressure calculated at the end of the second fluid time step has then retrieved accuracy and serves as input to the structure time step. While this method allowed us to technically compute with success the movement of the artificial valve nearly up to its closure, the analysis of the computation was not satisfying. In fact the valve acceleration presented a bad behavior, with a tendency to an exaggerated growth in time coupled with big drops at remeshing.

Positively impressed by the stability obtained by this splitting method, we have tried to fix the acceleration over each “two-time-step”. The result was that the valve acceleration became nearly continuous at remeshing and stabilized at a quite lower value than before. Unfortunately, after some remeshing procedures, the acceleration showed again a bigger oscillatory behavior and ended by being instable.

A successive pressure coupling algorithm has been developed which evaluates the “operative” pressure for computing of torque as the mean calculated pressure over the last two time-step. While more stable than the preceding algorithm, it does not allow to pursue the closure simulation up to the (near) end.

All these algorithm showed a constant improvement in stability. They are

all somewhat based on regularizing the pressure effects. This smoothing takes into account the past history of the pressure and is more needed as the leaflet closes and the flow goes sharper. We finally used a parameterized algorithm for which we introduce an “effective”  $P_{eff}$  pressure as a weighting between the measured pressure  $P_{mea}$  and the former “effective” pressure. This gives, with a computing notation:

$$P_{eff} = \alpha P_{mea} + (1 - \alpha) P_{eff} \quad (16)$$

where  $\alpha$  is the weight parameter and evolve in this simulation from an initial 0.7 to a final 0.1.

## 5 Numerical Results

The boundary inflow data are taken from from experimental measurement from the SORIN BICARBON aortic valve ([11]). We should stress the fact that while the geometry of the proximal aorta should give rise to an axial-symmetrical 2D simulation, the structure of the valve is only plane-symmetric and its movement is computed from a torque which would be zero in the axial-symmetrical case. So, we evaluated the inlet flux and velocity with the cylindrical configuration in mind, but we used instead the 2D planar Navier-Stokes equations. As already pointed out in the introduction, this approximation does not allow us to infer quantitative informations from the simulation. However, we think that we have caught the qualitative behavior and the experience with pressure coupling algorithm is essential for future 3D computations.

### 5.1 Numerical values

The results of the simulation presented here has been effectuated with the following numerical setting.

1. **Inlet velocity:** the profile of the inlet velocity is a forth order parabola whose maximal value is linearly evolving in time so as to reach the value of  $250mm.s^{-1}$  in  $4.10^{-2}s$ . It should be noted that only the total flux has been taken from Sorin data. The profile used is highly arbitrary and inaccurate for this simulation. More realistic profile should consider a progressive inversion of the flow from the border to the center of the aorta as is seen for the inversion of a flow in a pipe. However, due to the curvature of the proximal aorta, the reflux is highly asymmetric and should also presents a strong rotational component ([14]). Implementing such better inlet flows require to have a compatible initial velocity field and pressure field which complicate quite a lot the simulation and is left for subsequent improvements.
2. **Time step:** the time step has been taken constant during all sequences of execution without remeshing and changed from the value of  $5.10^{-5}s$

when the valve is fully opened at the beginning of the simulation up to  $10^{-6}$  near to the leaflet closure. Flow and pressure waves that used to happen with the former coupling algorithm at the change of time step are no longer quantitatively relevant. The choice of the evolution of the time-step allows to reach more rapidly and still with a good accuracy and a reasonable flow pattern the interesting part of the simulation when approaching to the valve closure by a few degrees. At this moment the leaflet velocity becomes quite high and the mesh degenerate more rapidly. A small time-step is then necessary to have time to capture the good flow pattern between each remeshing. The diminution of the time step could seem exaggerated but it is also due to the diminution of the parameter  $\alpha$ . In fact, the “effective” time step for the coupling algorithm is of order  $\frac{Dt}{\alpha}$ . It is therefore necessary to keep this value much smaller than the time between two remeshing.

3. **Mesh nodes:** Due to remeshing, the number of nodes is not constant, even when the boundary mesh is preserved. In fact, we used two families of mesh. One with about 11.000 nodes and the other with about 24.000 nodes for an open leaflet (see 2). These number fall by more than 50% near the closure because the boundary meshes have been created to behave well for a near-closing valve. The coarsest grids have been used at the beginning of the simulation and the finest ones at the end of the simulation.

A sum up of the simulation is given in the following table, the star in parenthesis (\*) in the first column indicates that a successive identical sequence has given rise to an instability.

Sequence Number	Mesh type	Dt s	$\alpha$ ad.	$\theta$ $d^\circ$	$\dot{\theta}$ $Rad.s^{-1}$	$\ddot{\theta}$ $Rad.s^{-2}$	Time s	element number
2	1	5e-5	0.7	49.42	11.070	537.39	.04315	10668
4	1	2e-5	0.7	32.11	26.618	1415.3	.06026	9324
4	1	1e-5	0.6	15.54	42.872	2565.7	.06877	7274
2	2	5e-6	0.5	12.27	46.377	2953.3	.070045	15226
3(*)	2	2e-6	0.4	6.22	53.975	4558.3	.072158	13158
1(*)	2	1e-6	0.3	4.46	56.754	5543.9	.072711	12320
2	2	1e-6	0.2	2.21	61.033	7373.2	.073379	11214
1(*)	2	5e-7	0.2	1.67	62.176	7691.4	.073531	10882
2	2	2e-7	0.1	0.98	63.586	6636.8	.073724	10432

## 5.2 Results analysis

We show, in the following figures (3,4,5), the evolution of position, angular velocity and angular acceleration of the leaflet. Closure is reached at 60 degrees.

As shown before, the angular acceleration is proportional to the torque exerted on the leaflet. While the global motion and velocity of the leaflet looks very good, it can be noticed some small irregularities of the angular acceleration. These irregularities are localized at the re-initialization of the mesh, which are

# Leaflet closure

Evolution of the angle

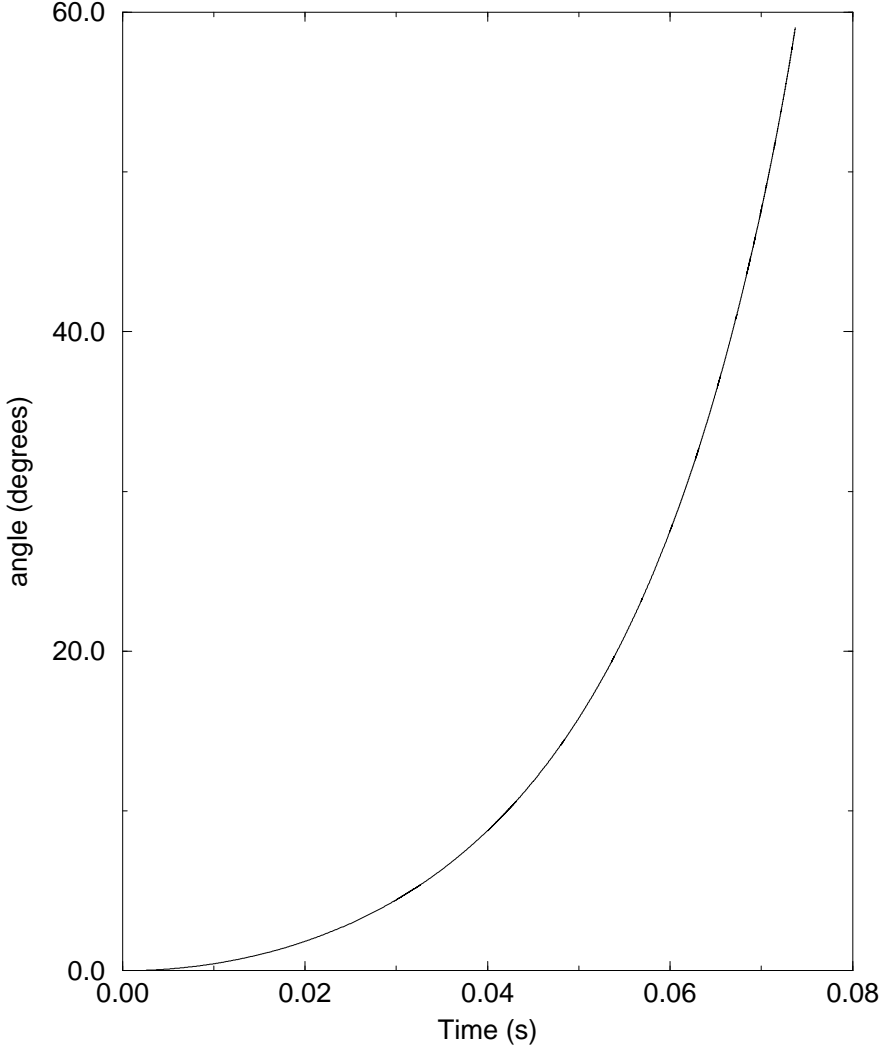


Figure 3:

more frequent as the valve closes. They are thought to be caused by the errors introduced during the interpolation and the flow takes some time to readjust itself in the good configuration. The jumps of pressure which have been cut to calculate the angular acceleration can be seen in figure (6).

The pressure drop induced by the leaflet is very small until few degrees of the closure and the simulation does not degenerate even at 1 degrees of the closure. The evolution of the mesh quality(fig.7) confirm the fact that degeneration of the mesh is faster when the leaflet boundary is closer to the external boundary.

It has been tried to diminish the time-step without altering the parameter  $\alpha$  when oscillations have appeared. No substantial gain of stability has been noticeable. The effect of  $\alpha$  is to delay the instantaneous information coming from the fluid over a characteristic time of  $\frac{Dt}{\alpha}$ , which is the real characteristic time from the accuracy point of view. This aspect should be correlated to coupling algorithms which use a global time step and then do sub-cycling on the separated fluid and structure parts, being implicit at the global level (see [6]). From this point of view, we use an algorithm totally explicit at the upper level. This is quite an important point, because it allows to do the coupling using the normal I/O data of any commercial code.

The value and location of the maximum shear stress are also plotted (8, 9). It can clearly be inferred from the figure (9) that the maximum shear stress near the time of closure is close to the axis of symmetry of the domain.

We also present the evolution of some relevant quantities with the variation of the leaflet angle:(10, 11, 12 and 13), and a temporal zoom over the end of the simulation: (14, 15, 16).

## 6 Conclusion

We have presented a fully coupled simulation of the fluid-structure interaction of the blood with a rotating leaflet. Due to large displacements, in spite of the ALE formulation, global remeshing is periodically done. The coupling algorithm used shows a very stable behavior, through the monitoring of a stabilizing parameter ( $\alpha$ ). It is nevertheless fully explicit and of easy implementation. The methodology and the technical main difficulties seem now under control, and full 3D accurate simulations can be expected in a near future.

## References

- [1] H. Zhang, M. Reggio, J.Y. Trépanier & R. Caramero, *Discrete Form of the CGL for moving meshes and its implementation in CFD schemes*, COMPUTERS FLUIDS VOL. 22, NO 1, PP. 9-23, 1993
- [2] K. Boukir, B. Nitrosso & B. Maury, *A characteristics-ALE method for variable domain Navier-Stokes equations*, HI-72/95/025/0 EDF-DER 1995

# Leaflet closure

Evolution of the angular velocity

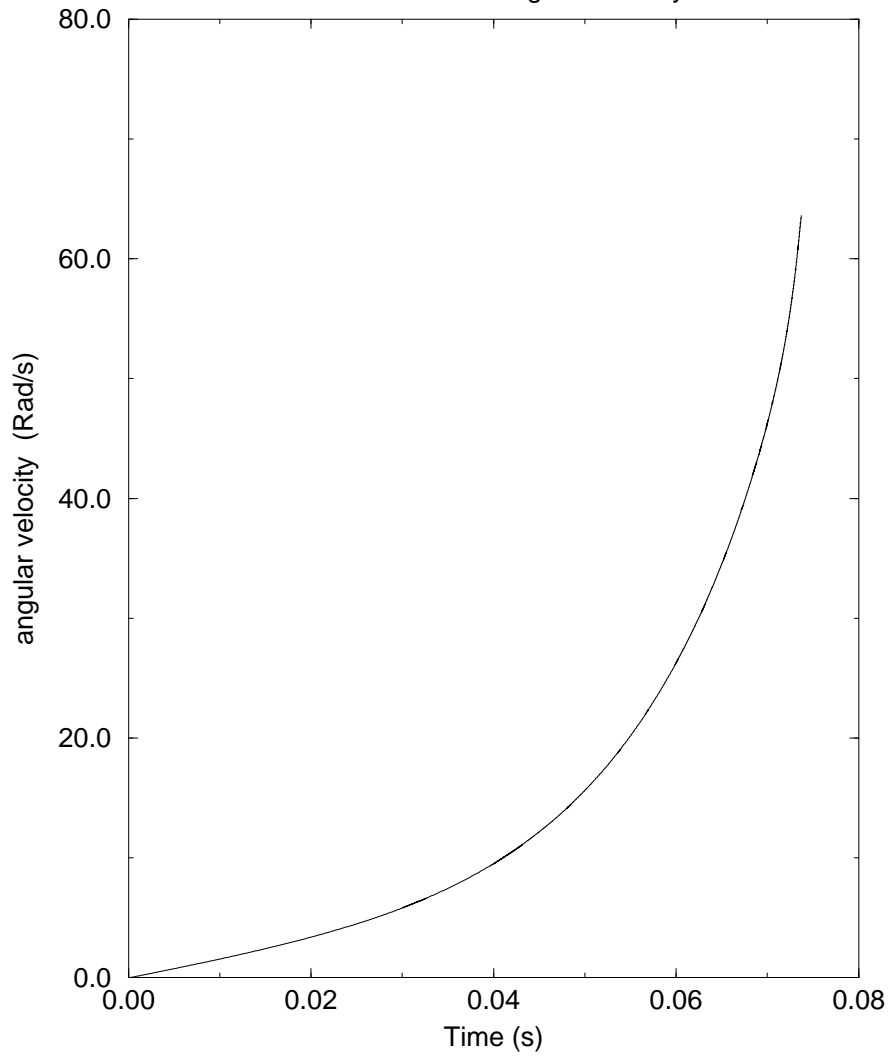


Figure 4:

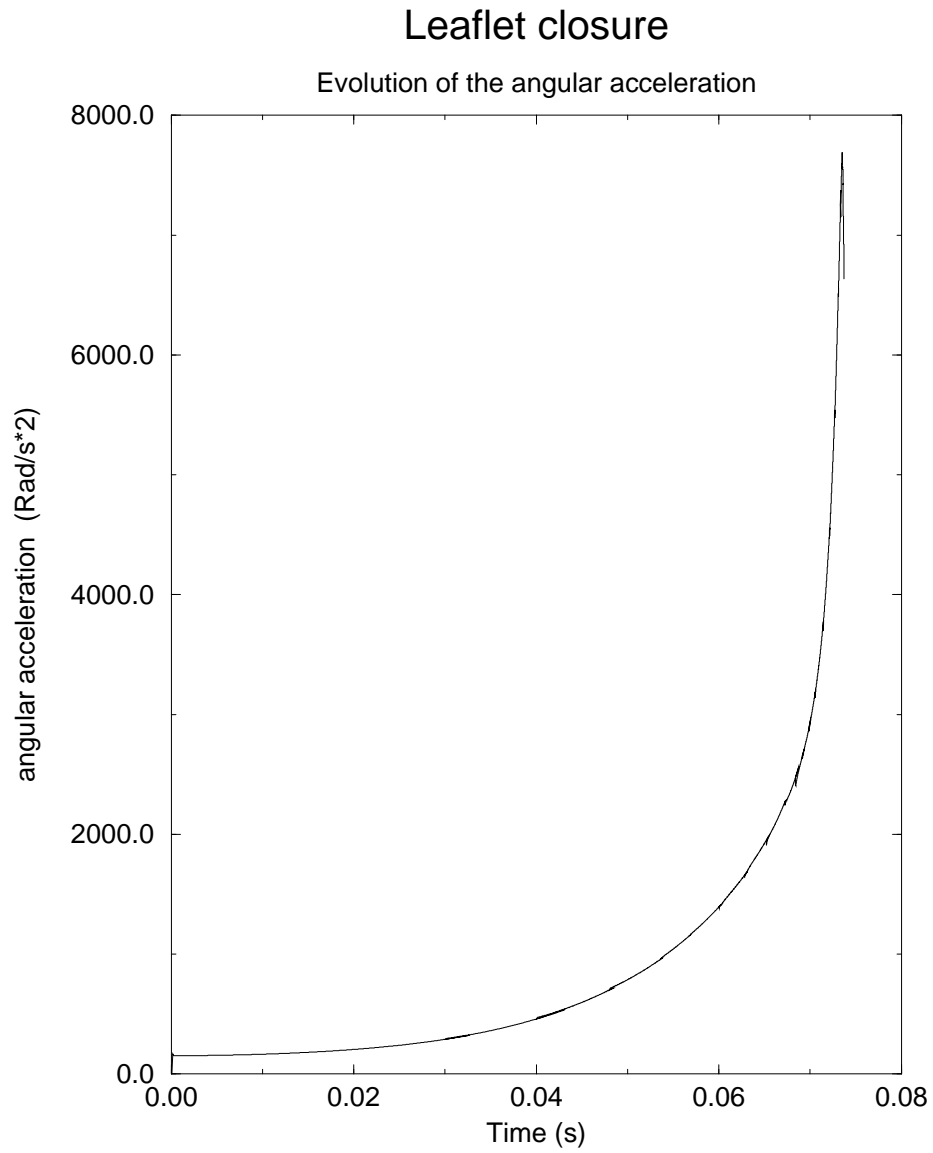


Figure 5: It can be seen that remeshing does not lead to any significant change of the angular acceleration of the leaflet. Moreover, the slopes are quite regular. The biggest discontinuity that can be seen around  $Time = 0.068s$  correspond to the change of mesh type.

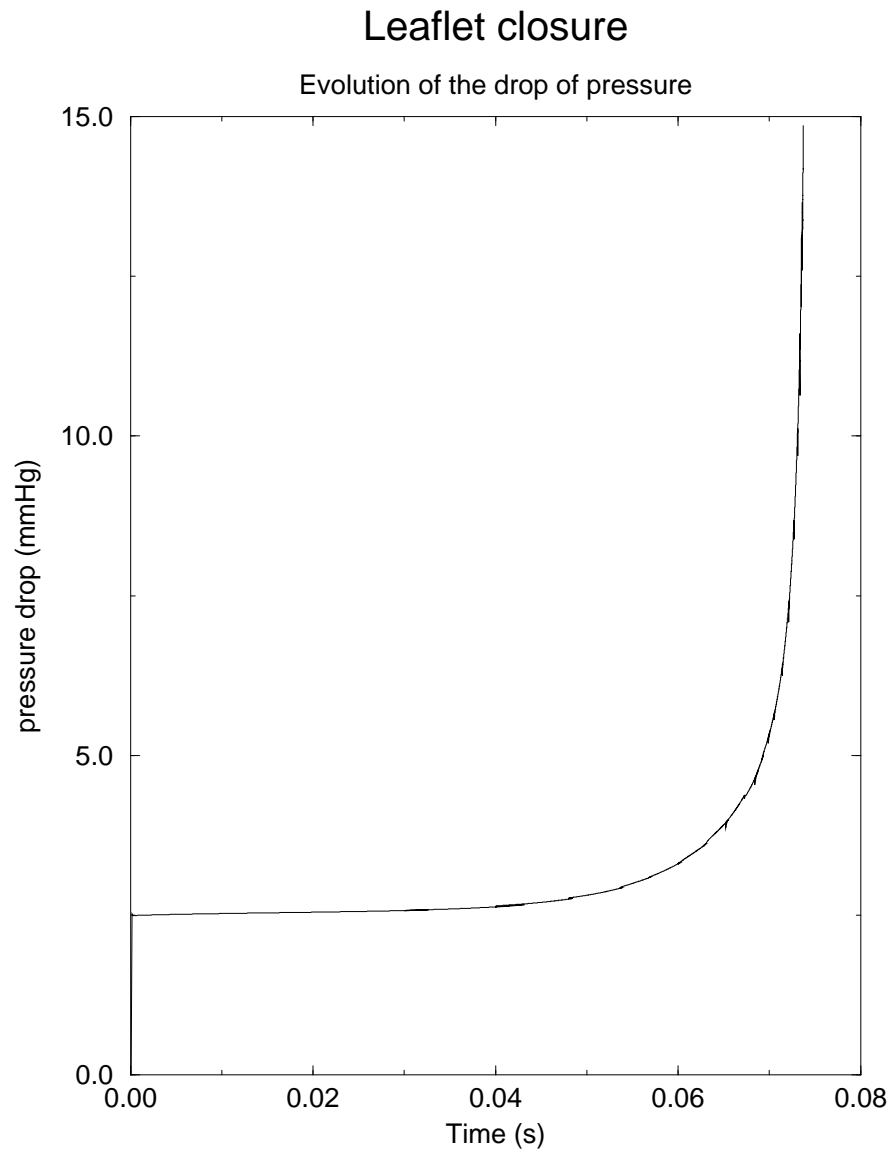


Figure 6: The total pressure drop across the computing domain takes essentially into account the forced kinetic acceleration in inlet. Effects due to the leaflet are progressively apparent to become dominant only near closure time

# Leaflet closure

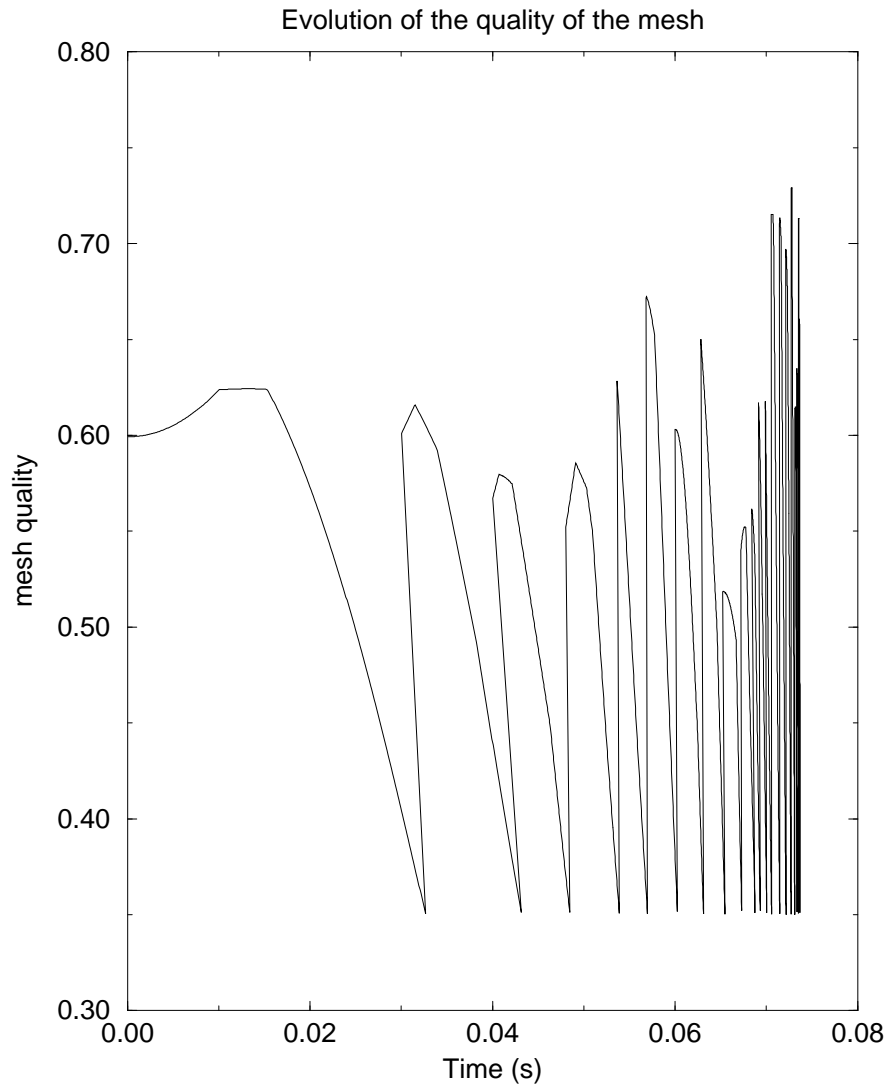


Figure 7: The evolution of the mesh quality forces to re-mesh at always smaller time intervals

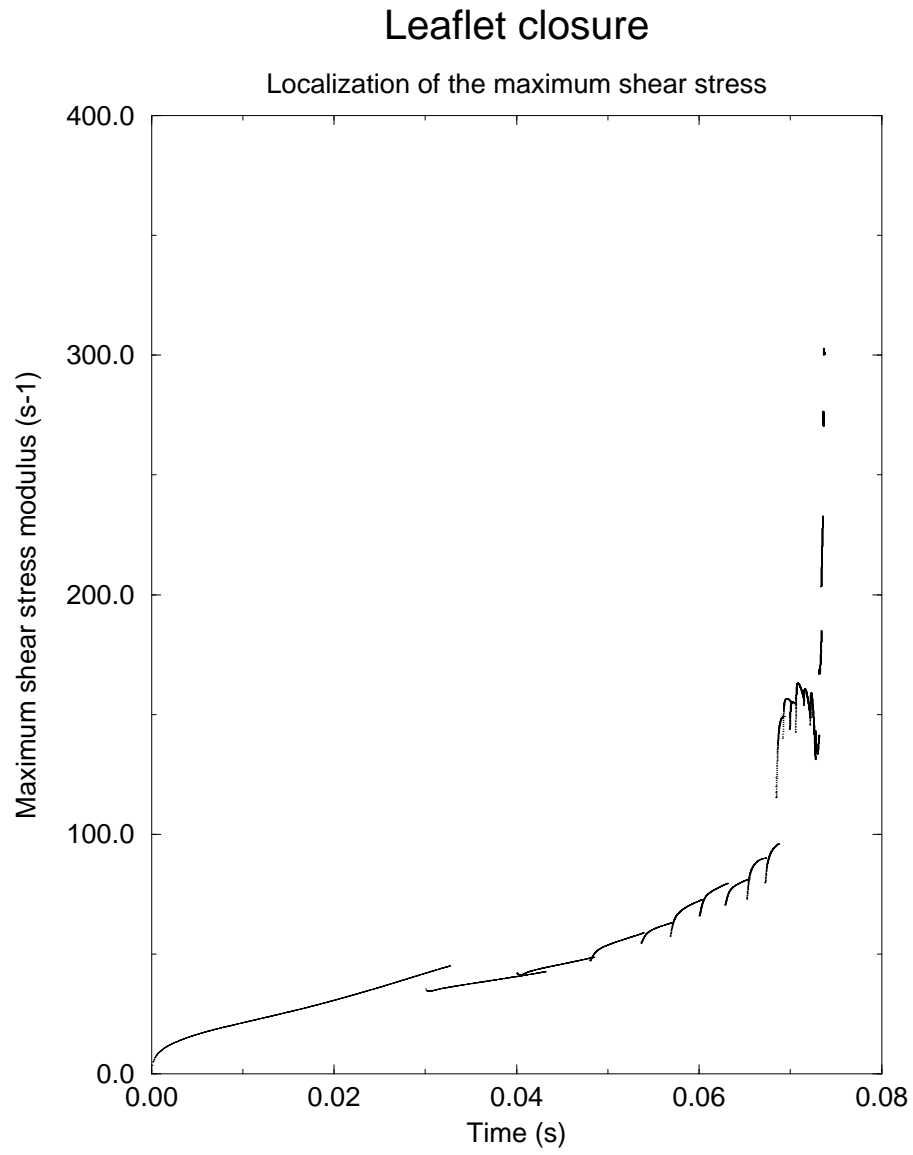


Figure 8: The evolution of the maximum shear stress is quite sensitive to the mesh regeneration. The change to a quite finer mesh at time  $t = 0.068s$  leads to a neat increase of the maximum value. This is an indication that the boundary layer, where it is localized, is not sufficiently refined.

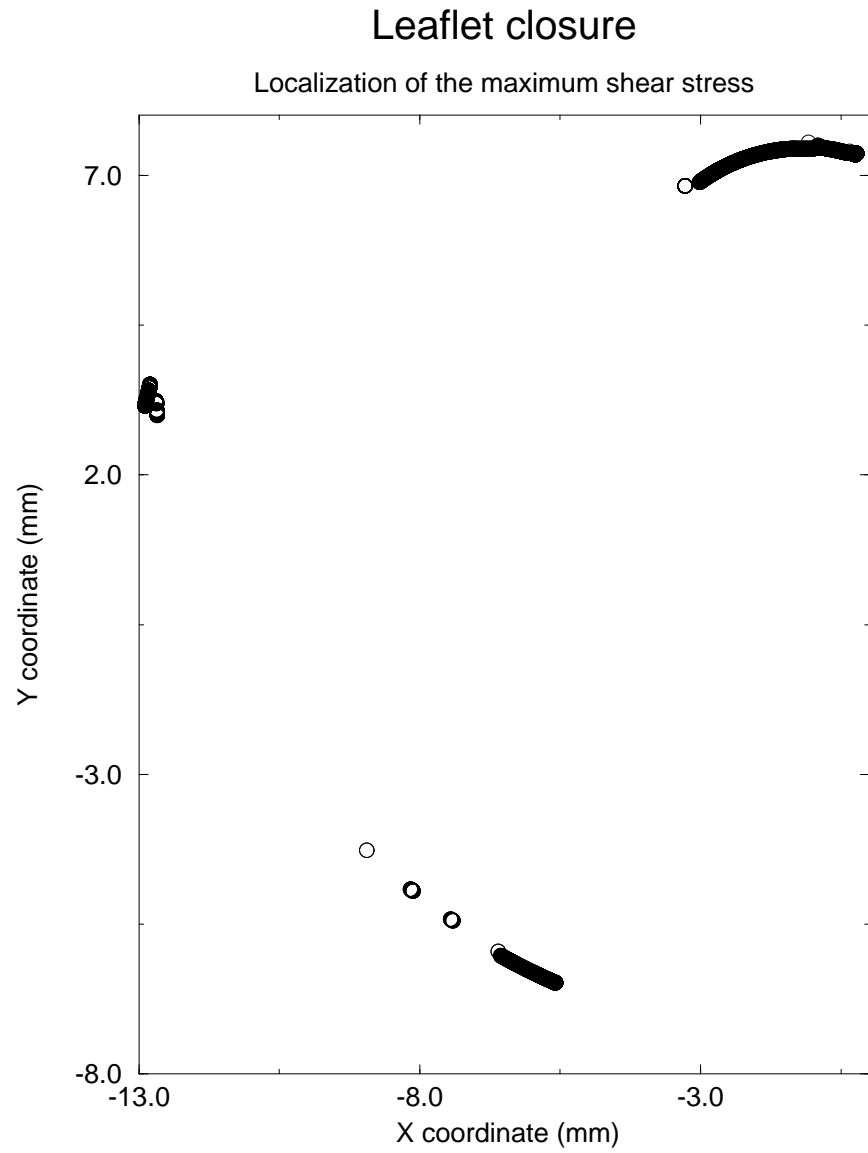


Figure 9: On this figure, we have plotted the position of the maximum shear stress during the simulation. The domain cover the computer fluid domain. Apart from the beginning of the simulation, the maximum shear stress is located on the leaflet boundary close to the symmetry axis.

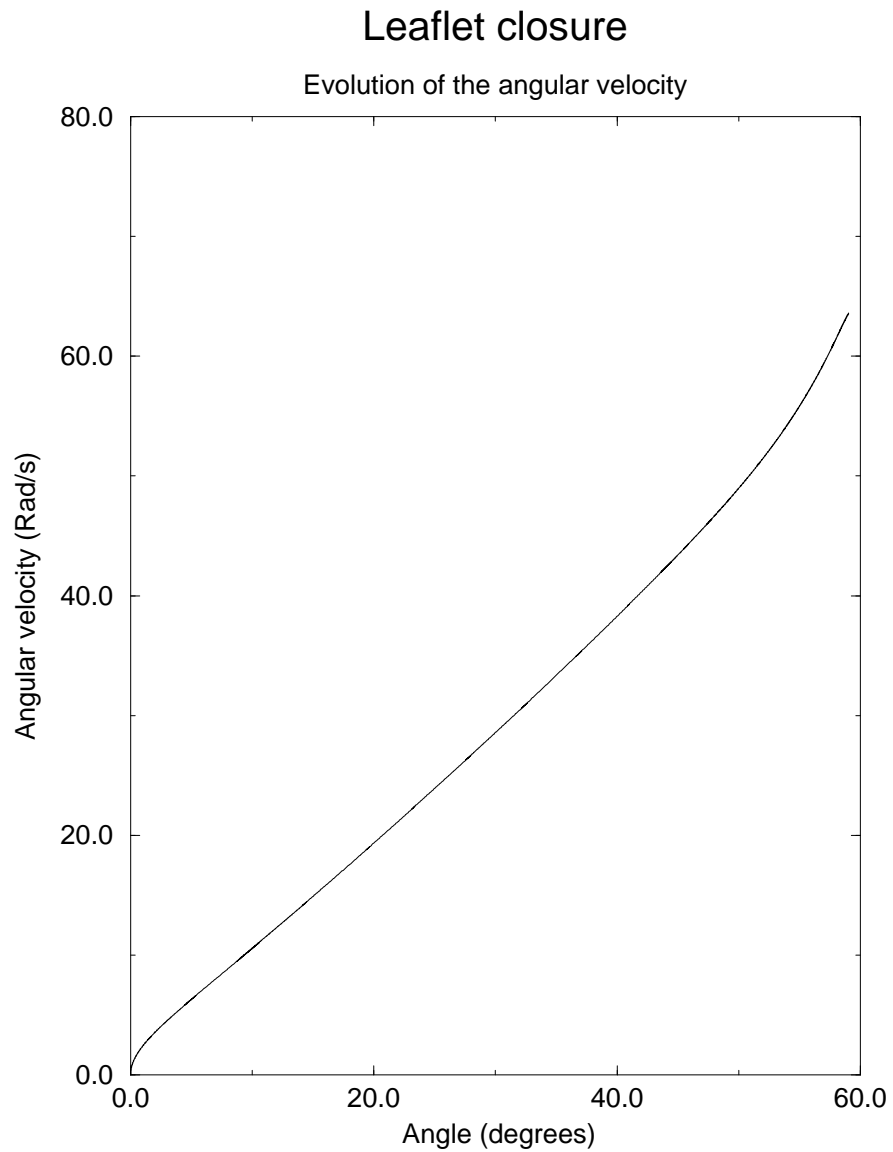


Figure 10: It can be seen that the angular velocity is increasing with the angle at a nearly constant rate over the quite large angular interval [3, 50].

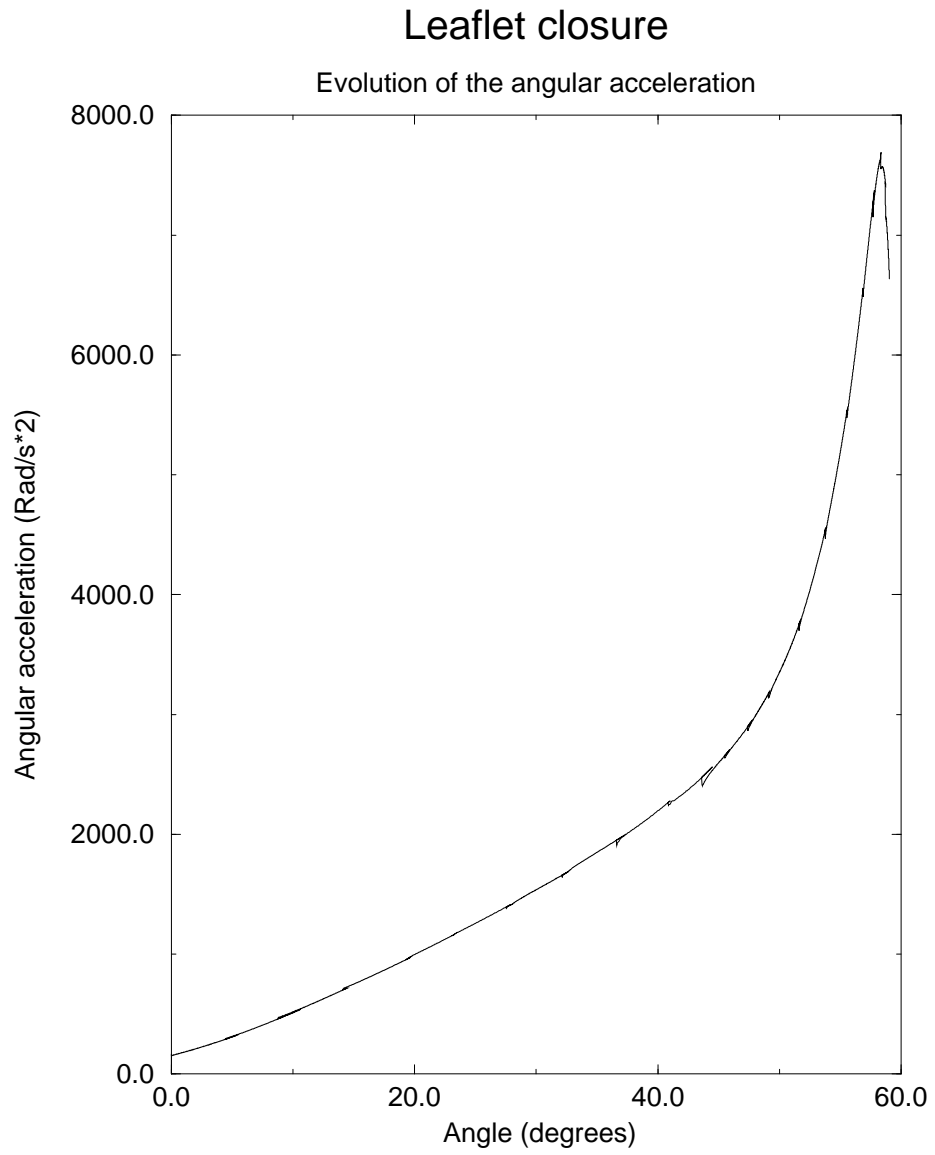


Figure 11: The leaflet is heavily accelerated along its path with a maximum around 2 degrees from the closure.

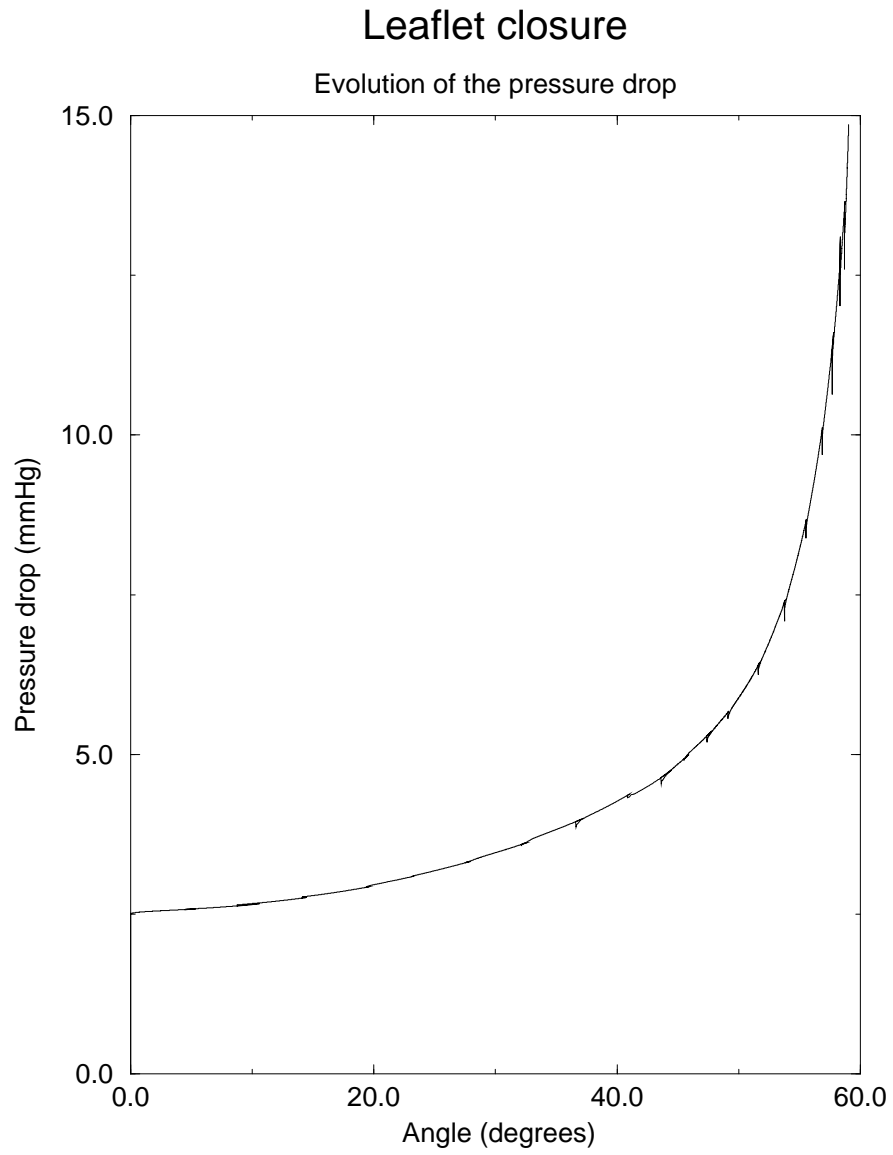


Figure 12: The effect of the leaflet for the pressure drop is significant only when been less than 10 degrees from the closure. The jumps of the pressure drop at remeshing increase quite a lot at the end of the simulation, indicating some lost in accuracy.

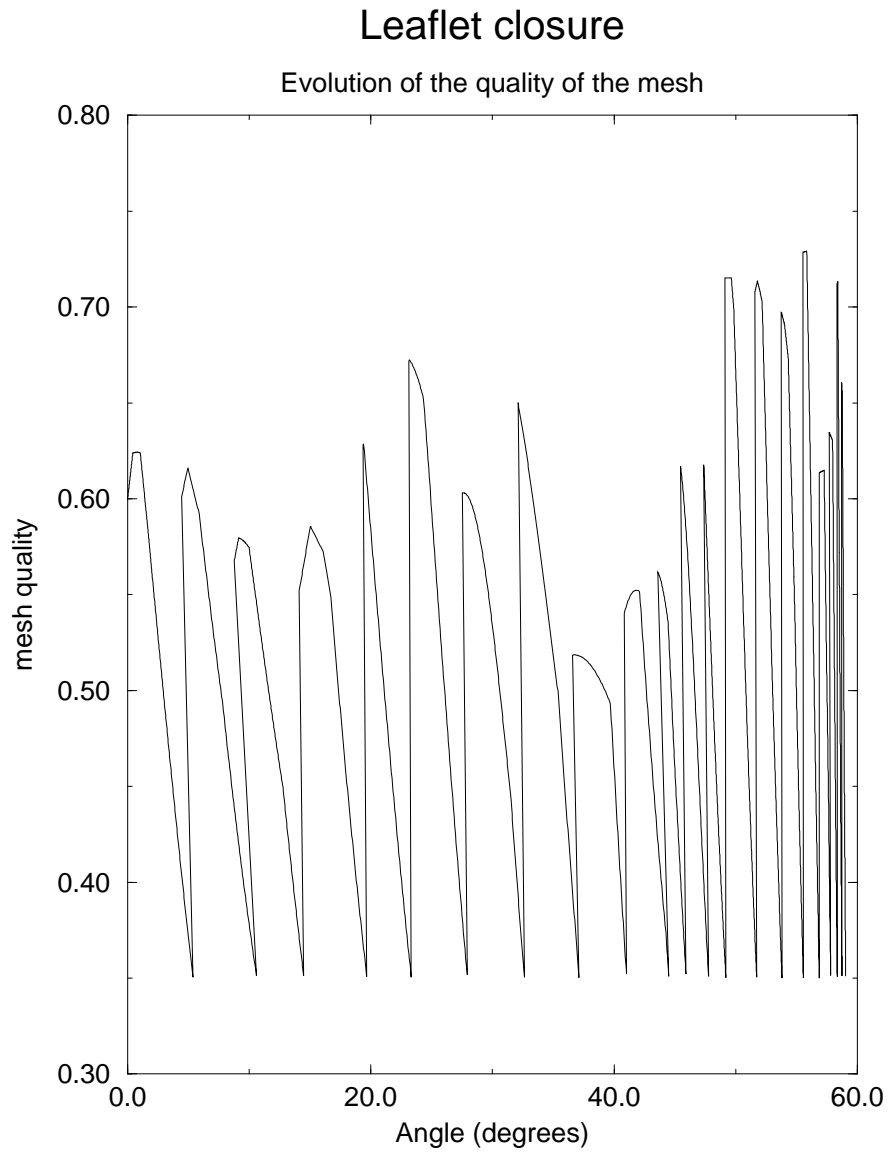


Figure 13: Remeshing becomes necessary more often near the closure of the leaflet because we are closer to a topological change of the domain.

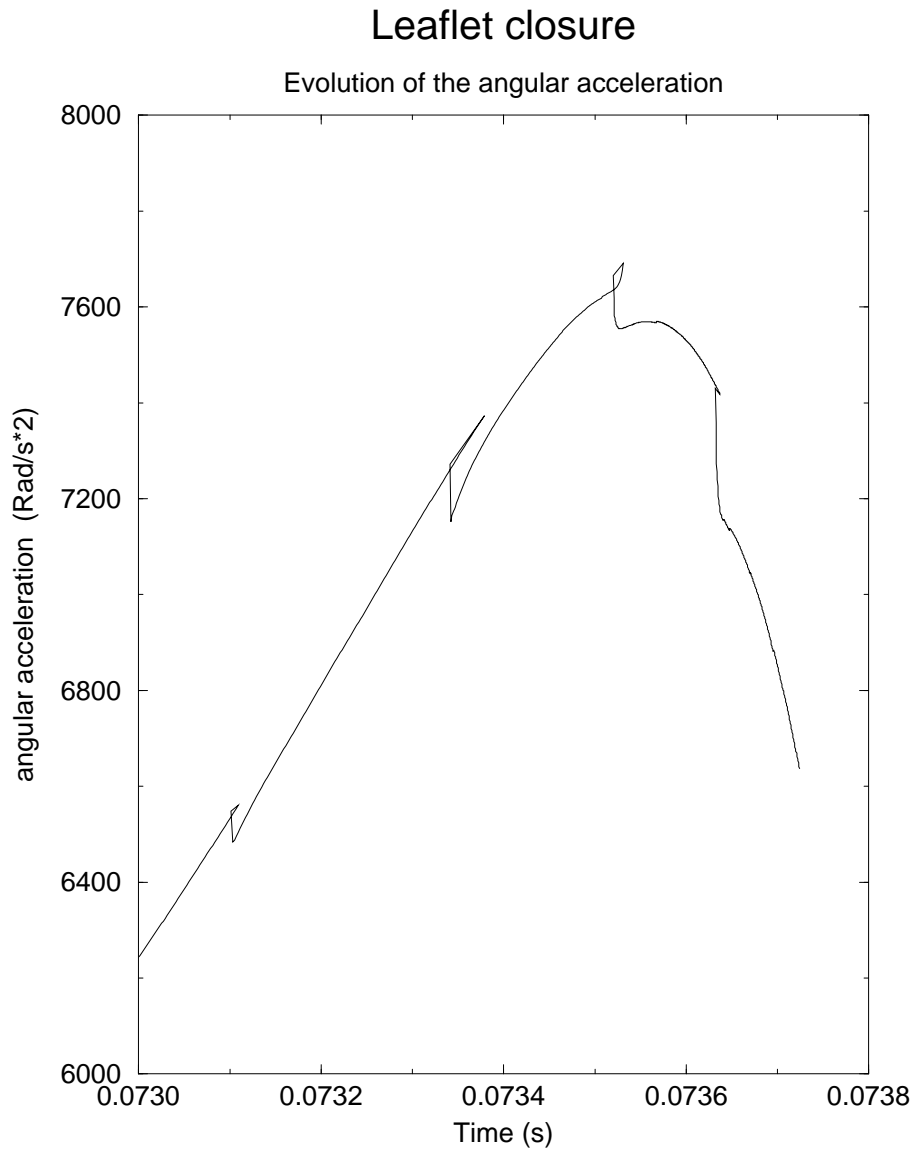


Figure 14: Only at the extreme end, we can see a lowering of the acceleration. It can also be noted the beginning of an instability at the maximum value. Fortunately the remeshing procedure took place a few time-steps before. Even at the extreme end of the simulation, the maximum jump in acceleration is less than 3 % . Note the time increment.

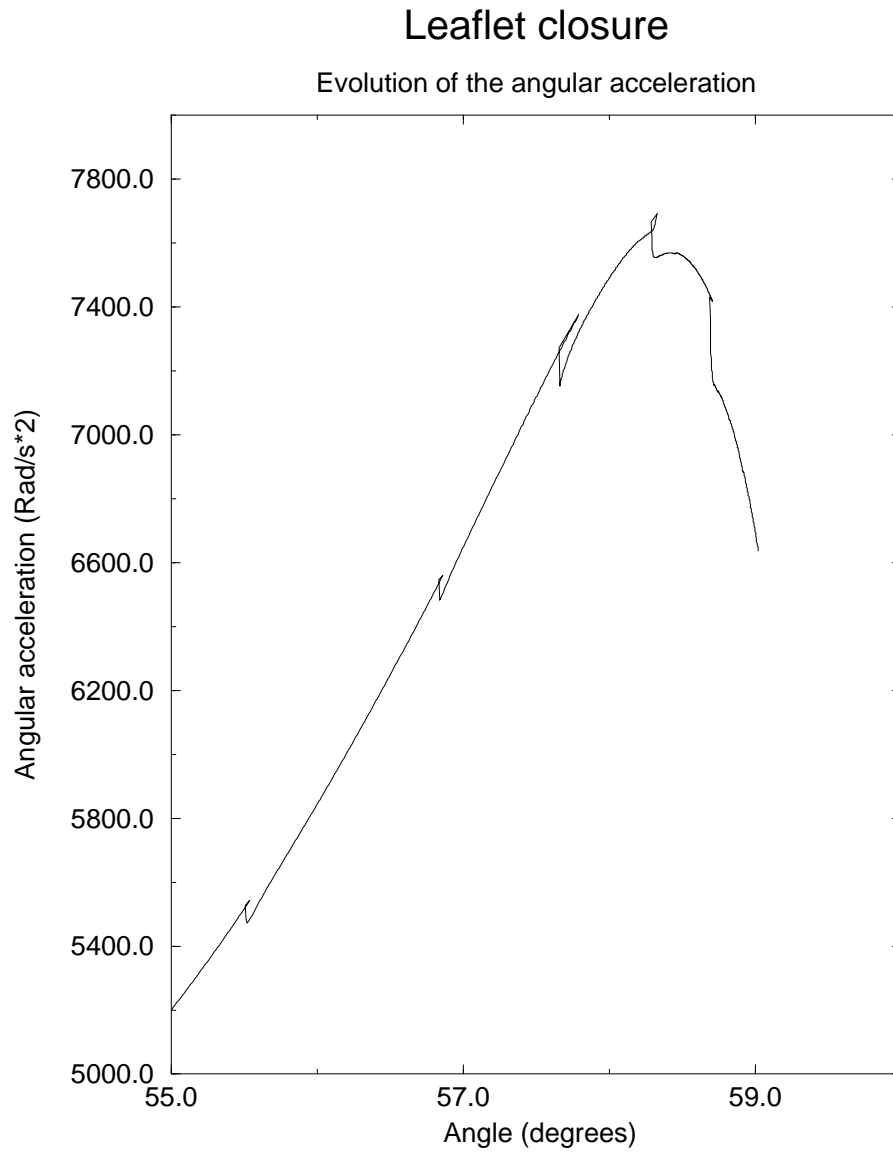


Figure 15: The acceleration increases by more than 50 % on the ultimate 4 degrees and then shows a small but stiff decreasing.

# Leaflet closure

Evolution of the drop of pressure

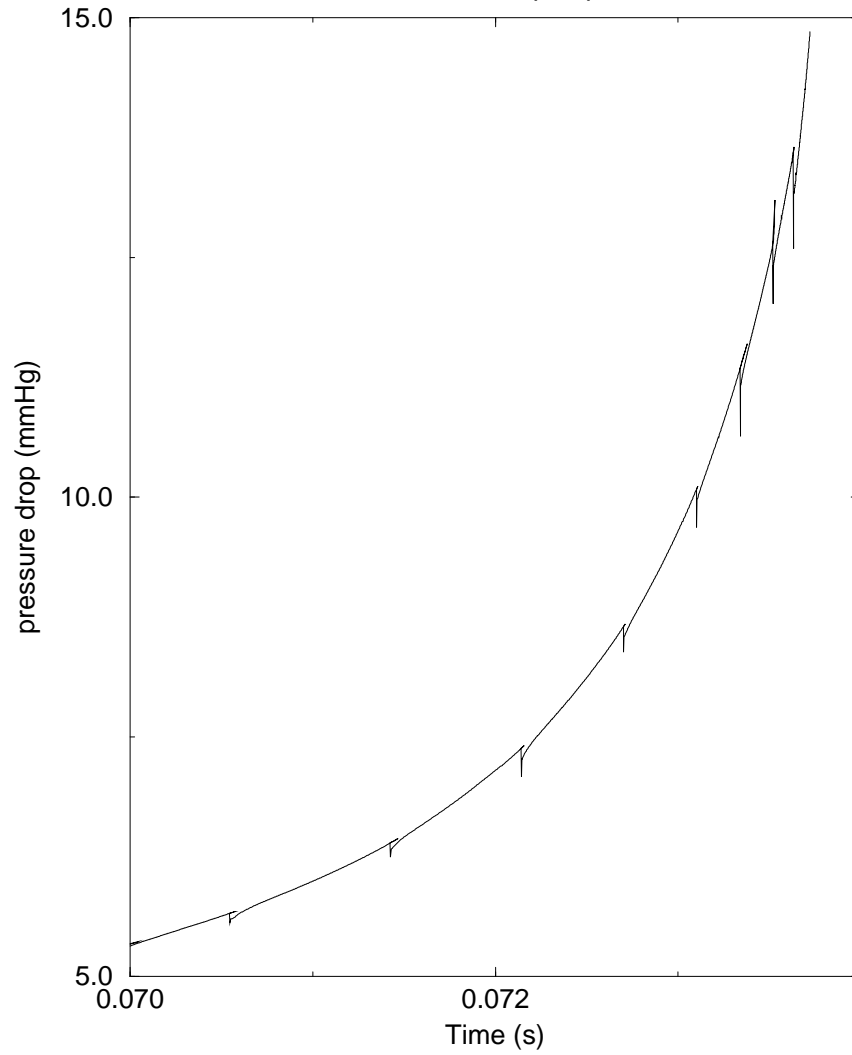


Figure 16: While becoming quite discontinuous at remeshing, the pressure drop increase until the end of the simulation.

- [3] C. Lacroix, B. Thomas & al., *Numerical simulation of fluid-solid interactions*, COPYRIGHT SIMULOG 1993 Réf : RAP.TS.93.CLS.004
- [4] B. Maury, *Formulation ALE et Méthode des Caractéristiques pour les Équations de Navier-Stokes avec Surface Libre*, Publication du Laboratoire d'Analyse numérique R93026, Université Pierre et Marie Curie.
- [5] J.Donea & S. Giuliani, *An explicit "ALE" finite element formulation for 3D transient dynamic fluid-structure interaction problems*, COMMISSION OF THE EUROPEAN COMMUNITIES Report 11936 EN (1989).
- [6] M.Lesoinne, C.Farhat & Nathan Maman, *Mixed explicit/implicit time integration of coupled aeroelastic problems: Three-field formulation, geometric conservation and distributed solution*, INT. J. NUM. METH. IN FLUIDS, VOL. 21, 807-835 (1995)
- [7] M.Lesoinne & C.Farhat, *Geometric Conservation Laws for Flow Problems with Moving Boundaries and Deformable Meshes, and Their Impact on Aeroelastic computations*, COMPUT. METH. APPL. MECH. ENGRG. (in press)
- [8] V.Moreau, *Arbitrary Lagrangian Eulerian (ALE) Formulation. Application for Euler and Navier-Stokes equations*, CRS4 Internal report(\*) (to appear)
- [9] V.Moreau, *A new linear interpolator, theory and motivation*. CRS4 Internal report(\*) (to appear)
- [10] C. Lacroix, C. Ibos, (SIMULOG) *Publication for AIAA 14th Aerodynamic Decelerator Systems Technology Conference* (SIMULOG, to appear)
- [11] G.Righini, (SORIN) *Personal communication*
- [12] K. Eriksson, D. Estep, P. Hansbo, C. Johnson, *Introduction to Adaptive Methods for Differential Equations. Acta Numerica (1995)*, pp.105-158
- [13] M. Fortin, M-G. Vallet, J. Dompierre, Y. Bourgault and W.G. Habashi, *Anisotropic Mesh Adaption: Theory, Validation and Application. ECCO-MAS 96*
- [14] Kilner PJ, Yang GZ, Mohiaddin RH; Firmin DN; Longmore DB; *Helical and retrograde secondary flow patterns in the aortic arch studied by three-directional magnetic resonance velocity mapping. Circulation, 1993 Nov, 88:5 Pt 1, 2235-47*
- [15] M. J. King, J. Corden, T. David and J. Fisher; *A three-dimensional, time-dependant analysis of flow through a bileaflet mechanical heart valve: comparison of experimental and numerical results J. Biomechanics, Vol.29, No. 5. pp. 609-618, 1996*
- [16] Peskin, C. (1992) *Cardiac fluid mechanics, chapter 17. Critical Reviews in biomedical Engineering 20, 451-459.*

(\*) pre-report down loadable on: <http://www.crs4.it/> moreau